A Stochastic Geometry Framework for Analyzing Pairwise-Cooperative Cellular Networks

Anastasios Giovanidis, François Baccelli

A Stochastic Geometry Framework for Analyzing Pairwise-Cooperative Cellular Networks

François Baccelli and Anastasios Giovanidis

***Abstract*—Cooperation in cellular networks is a promising scheme to improve system performance, especially for cell-edge users. In this work, stochastic geometry is used to analyze cooperation models where the positions of base stations follow a Poisson point process distribution and where Voronoi cells define the planar areas associated with them. For the service of each user, either one or two base stations are involved. If two, these cooperate by exchange of user data and channel related information with conferencing over some backhaul link. Our framework generally allows for variable levels of channel information at the transmitters. This paper is focused on a case of limited information based on Willems' encoding. The total per-user transmission power is split between the two transmitters and a common message is encoded. The decision for a user to choose service with or without cooperation is directed by a family of geometric policies, depending on its relative position to its two closest base stations. An exact expression of the network coverage probability is derived. Numerical evaluation shows *average coverage* benefits of up to 17% compared to the non-cooperative case. Various other network problems of cellular cooperation, like the fully adaptive case, can be analyzed within our framework.**

***Index Terms*—Cellular networks, Cooperative communications, CoMP, Coverage probability, Stochastic geometry**

I. Introduction

A promising idea in modern wireless network architecture is that of cooperative communications. Based on this, network nodes communicate with each other and try to adapt their transmission behavior in such a way that their own as well as the entire system performance is improved. Cooperation can be understood either as coordination of node actions after message passing, or as full cooperation by concurrent transmission of the same data towards a receiver node. The latter type requires full data and/or channel state information to be exchanged between the cooperating entities. In information theory, the idea originates from the Multiple Access Channel (MAC) with conferencing, whose capacity region was derived by Willems in [1] for the discrete memoryless case (also [2]) and by Bross et al. in [3] for its Gaussian extension.

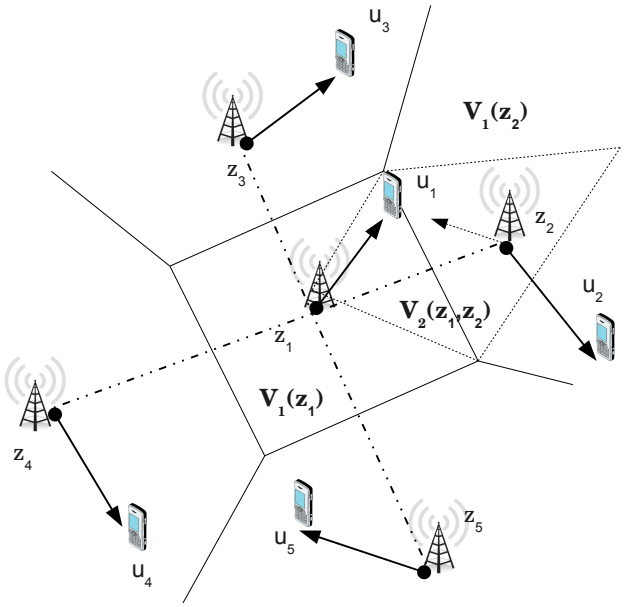

Fig. 1. Example of topology for a 5 BS network. The 1-Voronoi tessellation defines the cells. Neighbouring BSs share a 1-Voronoi boundary and exchange information over a backhaul link. The BSs can cooperate in pairs for the service of each user. In the figure, user $\mathbf{u}_1$ is located in the 1-Voronoi cell of BS $\mathbf{z}_1$ and the 2-Voronoi cell of the BS pair $(\mathbf{z_1}, \mathbf{z_2})$. Consequently, user $\mathbf{u}_1$ is considered primary user for $\mathbf{z}_1$ and secondary user for $\mathbf{z}_2$.

Focusing specifically on cellular architectures, a recent suggestion in 4G systems and beyond has been the Cooperative MultiPoint transmission (CoMP) [4], [5]. With the use of appropriate precoding, interference within a so called Base Station (BS) cooperation cluster can be cancelled out for the users in service. The concept is also known in the literature as Network MIMO [6]. A 2-transmitter 2-receiver CoMP model is investigated in [7] and an achievable rate region is derived from the Willems' capacity region, when each BS sends a private and a common message to both receivers. Practical schemes to implement cooperation, combining private/common message and Dirty Paper Coding can be found in [8].

Benefits from cooperation come however at a cost for the network. The grouping of BSs may require that information over the (local or global) channel quality be made available at a central controller, who defines the cooperation sets, called clusters [9]. Alternatively, dynamic clustering mechanisms require a considerable exchange of information among net-

The work presented in this paper has been carried out at LINCS (http://www.lincs.fr) and has been supported by INRIA and LINCS, Paris, France. Part of the results have been presented at the 47th Annual Asilomar Conference on Signals, Systems, and Computers, Pacific Grove, California USA, 3-6 November 2013.

François Baccelli holds the Simons Chair in Mathematics and Electrical and Computer Engineering, UT Austin, Wireless Networking and Communications Group, 2501 Speedway Stop C0806, Austin, Texas 78712-1687, USA. He is also affiliated with INRIA Rocquencourt and ENS Paris, team DYOGENE (former TREC), 23 avenue d'Italie, CS 81321, 75214 Paris, France.

Anastasios Giovanidis was with INRIA Rocquencourt and ENS Paris, team DYOGENE (former TREC). He is now with the French National Center for Scientific Research (CNRS), LTCI laboratory, Télécom ParisTech, 23 avenue d'Italie, 75013 Paris, France.

work BS's as well [10], [11]. Furthermore, the full benefits of cooperation are known to be achieved when both data and channel state information are fully known to all the transmitters in a cluster [6]. In such a case, optimal resource allocation is possible [12]. Such information exchange requires however considerable feedback, which is often unrealistic because of the system resources necessary to be reserved and of limitations on backhaul capacity [13]. Approaches to overcome the problem consider schemes of partial, delayed or quantized channel information exchange between the cooperating entities [14], [15] as more realistic towards a practical system implementation.

The existing research, as shown above, has been restricted to two types of models: either those with a small number (usually two) of cooperating transmitters and one or more receivers, or those with fixed cellular architectures such as the Wyner model or the hexagonal grid. However, both ways to analyze a communications network are incomplete. The former, because it ignores the effect of out-of-cluster interference. The latter because it does not account for the random planar deployment of BSs - although both are useful as simple geometrical models and simulation settings. In this work we aim at analyzing the performance of cooperation using the tools of stochastic geometry, which can on the one hand model an infinite planar network, while on the other exhibit the necessary randomness in the BS positioning. Such an approach has already been proven valuable in deriving closed form expressions for the coverage of standard as well as K-tier cellular networks, as shown in the works of Andrews *et al* in [16] and Dhillon *et al* in [17] respectively. Recently, the assumption of Poisson distribution for the BS positions seen by a typical user, has been verified by Błaszczyszyn *et al* to hold for a large variety of networks with log-normal shadowing [18].

A. Related work to the spatial model of cellular cooperation

The present paper deals with the question of coverage when BSs cooperate in neighbouring pairs and compares the performance of the scheme with the standard non-cooperative architecture. Very recently and parallel to the authors' work, several contributions have appeared on the same subject, where different system models, approximations, bounds and tools have been developed to analytically solve the CoMP network performance problem. A first effort with a random number of cooperating BSs is found by Akoum and Heath in [19]. In this, the hierarchical model is applied and disjoint random-sized clusters are formed, whose BSs are equipped with multiple antennas and transmit using intercell interference nulling. Another approach with a random number of cooperating BSs in hexagonal-shaped hierarchical clusters is found in Huang and Andrews [20], where the authors analyze the asymptotic behaviour of the outage probability when the cluster size increases unboundedly, using large deviations.

Following our work (presented already in [21]), we find the approach by Nigam *et al* [22], which considers user-defined cooperation between BSs that may belong to different tiers of a heterogeneous network. The scheme is based on joint transmission and signal powers add-up as a new exponential random variable at the user side. The authors derive the cooperation coverage gain when a user receives service either by the set of strongest BSs of each tier or the set of overall n BSs with the strongest sum, while the rest create interference. Related to user-defined cooperation Tanbourgi *et al* recently proposed the joint transmission cooperation of all BSs lying within a circle of some radius around the typical user, and derive the non-coherent CoMP performance in [23]. Finally, Błaszczyszyn and Keeler in [24] present a general result on the SINR outage probability with the use of factorial moment measures, when any possible set of BSs combine their independent signals to serve the typical user by cooperation, successive interference cancellation or other alternative technique.

In our work we analyse a simpler model with cooperation in pairs but provide accurate coverage expressions and tuneable cooperation policies. Furthermore, although the analysis focuses on the performance evaluation at the typical location, we carefully consider how resources of interfering BSs are distributed to serve the other users of the network. The modelling and analysis, here, aims at providing a *general framework* to treat problems of user-defined cooperation that can potentially be extended to larger cluster cardinalities.

B. Contributions

The main contributions of our work are summarized below:

i) We consider single-antenna BSs distributed on the plane as a Poisson Point Process (PPP) with a predefined intensity λ. The network BSs are understood as a pool of resources where all users have access to, depending on each one's position. Using the tools of stochastic geometry, we analyze a user-defined cooperation scheme, where a user can choose to receive service by one or two BSs, i.e. its first and second closest geographic neighbour (see Fig.1 and Section II). The relative user position is important and is related to the Voronoi tessellation of the plane.

ii) A novel cooperation policy is introduced, which triggers cooperation only when the user lies inside a planar zone at the cell borders (Section II.B). The zone has a width, tuneable by a parameter ρ.

iii) We analyze a cooperation scheme with limited information exchange between BSs. The scheme evaluated, uses the concept of Willems' encoding [1] or equivalently beamforming with partial channel state information (CSI) over the channel phase (Section II.A and II.C).

iv) Our model treats all cells and users of the network equally and compares the performance in the case of cooperation and of no cooperation in a fair way. Specifically, the same number of users is served in both cases. Additionally, the power consumed per user by the network is equal in both cases.

v) We evaluate the coverage probability of the network (in Section III) and provide expressions in integral form, which can be numerically evaluated.

vi) A modification of the scheme considers knowledge over the intra-cell interference for the cooperating pair. Such interference is due to the fact that in our model each pair may serve more than one users. By application of Dirty Paper

Coding (DPC) orthogonal transmission of the beneficial signal to this interfering signal, provides coverage benefits over the entire SINR threshold domain (Section IV). The cost is the extra information over this interfering signal.

vii) We explicitly explain the pros and cons of the co-operation scheme (Section V), provide numerical evaluation and comparison with simulation results (in Section VI) and conclude our work with a discussion on future extensions (Section VII).

In summary, the coverage benefits from the cooperation scheme with limited CSI reach up to 10% without, and 17% with DPC. We verify hence that, although the absolute gains are not immense, the scheme does improve coverage at the edges of the cells. Additional notes on our model can be found in Appendix A. Proofs of theorems not included in the main text are given in the Appendices B-D.

Notation: We will use capital letters G for random variables (r.v.'s), boldface small letters $\mathbf{x}$ for vectors (including planar points) and small letters a for real/complex quantities. Capital calligraphic letters are reserved for sets (except for the notation on signal $\mathcal{S}$ and interference $\mathcal{I}$). The set of real numbers will be denoted by $\mathbb{R}$ and that of complex numbers by $\mathbb{C}$. The unit imaginary number is denoted by $j := \sqrt{-1}$. The asterisc notation a^* denotes the complex-conjugate of $a \in \mathbb{C}$. The distance between two planar points $\mathbf{z}$ and $\mathbf{u}$ is denoted by $d(\mathbf{z}, \mathbf{u})$.

II. Cooperation in the Network under Study

For the model under study, the BSs are equipped with a single antenna and are positioned at the locations of atoms from the realization of a planar PPP with intensity λ, denoted by $\phi = \{\mathbf{z}_i\}$. A planar tessellation, called the 1-Voronoi diagram [25], [26], partitions (up to Lebesgue measure zero) the plane into subregions called cells. The *1-Voronoi cell* $\mathcal{V}_1(\mathbf{z}_i)$ associated with $\mathbf{z}_i$ is the locus of all points in $\mathbb{R}^2$ which are closer to $\mathbf{z}_i$ than to any other atom of ϕ. We consider Euclidean distance $d(\mathbf{z}_i, \mathbf{z})$.

$$\mathcal{V}_1(\mathbf{z}_i) = \left\{\mathbf{z} \in \mathbb{R}^2 |\ d(\mathbf{z}_i, \mathbf{z}) \leq d(\mathbf{z}_j, \mathbf{z}), \forall \mathbf{z}_j \in \phi \setminus \{\mathbf{z}_i\}\right\}. \quad (1)$$

When the 1-Voronoi cells of two atoms share a common edge, they constitute *Delaunay neighbours* [26]. A dual graph of the 1-Voronoi tessellation, called the Delaunay graph, is constructed if all Delaunay neighbours are connected by an edge. The 2-Voronoi diagram [25] consitutes another partition (up to Lebesgue measure zero) of the plane. Specifically, the *2-Voronoi cell* $\mathcal{V}_2(\mathbf{z}_i, \mathbf{z}_j)$ associated with $\mathbf{z}_i, \mathbf{z}_j \in \phi$, $i \neq j$ is the locus of all points in $\mathbb{R}^2$ closer to $\{\mathbf{z}_i, \mathbf{z}_j\}$ than to any other atom of ϕ:

$$\begin{aligned}\mathcal{V}_2(\mathbf{z}_i, \mathbf{z}_j) \quad = \quad & \left\{\mathbf{z} \in \mathbb{R}^2 |\ d(\mathbf{z}_i, \mathbf{z}) \leq d(\mathbf{z}_k, \mathbf{z}) \ \ \& \right. \\ & \left. d(\mathbf{z}_j, \mathbf{z}) \leq d(\mathbf{z}_k, \mathbf{z}), \forall \mathbf{z}_k \in \phi \setminus \{\mathbf{z}_i, \mathbf{z}_j\}\right\} \quad (2)\end{aligned}$$

It can easily be shown that this new 2-Voronoi tessellation covers the 2D space. Staring by any planar point, we can open a ball around it and let its radius grow, until one atom of the PPP lies inside the ball and another one (or two or max three) on its boundary, or until two (or max three) atoms fall on its boundary and the interior is empty. Observe here, that in the PPP case, the event that more than three atoms are co-circular has zero probability. Then this point will either be an interior point of exactly one 2-Voronoi cell, or it will be a boundary point between two 2-Voronoi cells, or a vertex of three cells. The 2-Voronoi cell of a homogeneous PPP is a convex set (since it is defined as the intersection of half-planes), and compact [25].

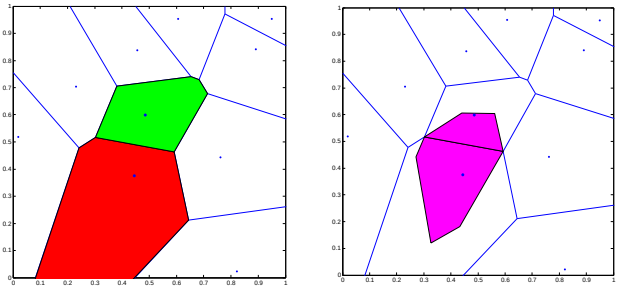

(a) 1-Voronoi tessellation example. (b) 2-Voronoi tessellation example.

Fig. 2. Illustration example for the 1- and 2-Voronoi tessellations in a square with area 1 $[m^2]$, based on the uniform positioning of 10 atoms. The subregions highlighted refer to a specific pair of atoms.

We consider a geometric cooperation scenario based on four assumptions. (a) Each BS is connected via backhaul links of some sufficient capacity for the scheme, with all its Delaunay neighbours. No questions on infrastructure will be treated in our work. (b) Exactly one user with a single antenna is initially associated with every BS. Each user is located randomly at some point within the 1-Voronoi cell of its BS and we write $\mathbf{u}_i \in \mathcal{V}_1(\mathbf{z}_i)$ with known coordinates. Because of this choice, the user positions do not follow a PPP distribution. (c) Each user $\mathbf{u}_i$ may be served by either one or two BSs. If two, these correspond to the atoms of ϕ which are its *first* and *second closest geographic neighbour*. If one, it is just the first closest neighbour. We use the notation $\mathbf{b}_{i1}$ and $\mathbf{b}_{i2}$ when referring to these neighbours. By definition the user belongs to $\mathbf{u}_i \in \mathcal{V}_2(\mathbf{b}_{i1}, \mathbf{b}_{i2})$. (d) From the point of view of a BS located at $\mathbf{z}_i$, we refer to the user in its 1-Voronoi cell as the *primary user* $\mathbf{u}_i$ and to all other users served by it but located outside the cell as the *secondary users*. These constitute a set $\mathcal{N}^s(\mathbf{z}_i)$, with cardinality that ranges between zero and the number of Delaunay neighbours of $\mathbf{z}_i$, and which depends on the users' position relative to $\mathbf{z}_i$.

The distance between user $\mathbf{u}_i$ and its first and second closest BS neighbour is equal to $d(\mathbf{b}_{i1}, \mathbf{u}_i) = r_{i1}$ and $d(\mathbf{b}_{i2}, \mathbf{u}_i) = r_{i2} \geq r_{i1}$. The second nearest BS $\mathbf{b}_2$ can only be one of the Delaunay neighbours of $\mathbf{b}_1$. The cooperation scenario with the notation introduced is shown in Fig. 1. An example of 1- and 2-Voronoi tessellation is shown in Fig. 2(a) and 2(b).

A. Pairwise Cooperation: Willems' Encoding, Power Splitting and In-Phase Transmission

Our communications scheme applies the following idea. When two BSs cooperatively serve a user in the downlink, its signal is split into one *common part* served by both, and

private parts served by each one of the serving BSs. The common part contains information known to both transmitters, that is exchanged between them over a reliable conferencing link [1], [3], [7], [8], [27]. Concerning channel knowledge, we assume that only the information on the channel phase shift is available at the transmission pair (together with information over the interference from the base station pair, in the DPC case later in our work), so that full adaptation of the signal to the instantaneous channel conditions is not possible. More specifically, for each primary user $\mathbf{u}_i$ located within the 1-Voronoi cell of atom $\mathbf{z}_i$, consider a signal $s_i \in \mathbb{C}$ to be transmitted. The user signals are independent realizations of some random process with power $\mathbb{E}\left[|s_i|^2\right] = p > 0$ and are uncorrelated with other user-signals meaning $\mathbb{E}[s_i s_n^*] = 0$, $\forall n \neq i$. The signal destined to user $\mathbf{u}_i$ in the downlink is split into $s_i = s_i^{(p)} + s_i^{(c)}$.

- A *private* part sent to $\mathbf{u}_i$ from its first BS neighbour $\mathbf{b}_{i1} := \mathbf{z}_i$, denoted by $s_i^{(p)}$. The second neighbour does not have a private part to send.

- A *common* part sent by both $\mathbf{b}_{i1}$ and $\mathbf{b}_{i2}$, which is denoted by $s_i^{(c)}$. This part is communicated between both BSs over the backhaul links.

The two parts are uncorrelated random variables, in other words $\mathbb{E}\left[s_i^{(p)} s_i^{(c)*}\right] = 0$. For clarity purposes, we will use the notation $s_i^{(c1)}$ for the common signal at $\mathbf{b}_{i1}$ and $s_i^{(c2)}$ for the common signal at $\mathbf{b}_{i2}$, although the two are versions of the same signal $s_i^{(c)}$ transmitted by different BSs.

Considering power issues, we put the constraint that the powers transmitted from both BSs to serve user $\mathbf{u}_i$ should sum up to p to guarantee *power conservation*. This is similar to the beamforming normalization, found in [7]. We assume that the common part is served by both BSs with the same power percentage $a_i \in \left[0, \frac{1}{2}\right]$, which is named the *power-split-ratio*.

$$\mathbb{E}\left[\left|s_i^{(p)}\right|^2\right] = (1-2a_i)\,p, \mathbb{E}\left[\left|s_i^{(c1)}\right|^2\right] = \mathbb{E}\left[\left|s_i^{(c2)}\right|^2\right] = a_i p.$$

We denote the infinite vector of these ratios by $\mathbf{a}$ and the vector of ratios omitting the entry a_i, by $\mathbf{a}_{-i}$. Then, BS $\mathbf{b}_{i1}$ consumes $(1-a_i)\,p$ in total for user $\mathbf{u}_i$, while BS $\mathbf{b}_{i2}$ consumes $a_i p$ for the same user. Each BS $\mathbf{z}_i$ transmits a total signal x_i. By applying superposition coding [28], [8], this signal consists of the private and common message for its primary user $s_i^{(p)} + s_i^{(c1)}$ and the common message for all its secondary users $s_k^{(c2)}$, $k \in \mathcal{N}^s(\mathbf{z}_i)$,

$$x_i = s_i^{(p)} + s_i^{(c1)} + \sum_{k \in \mathcal{N}^s(\mathbf{z}_i)} s_k^{(c2)}. \quad (3)$$

We can use superposition coding, since we generally expect at most two secondary users scheduled per BS, in which case the decoding performs well. It can be shown that the probability of more than two secondary users asking for service by the same BS is close to zero (≈ 0.065). For rare events with larger number of users, we assume an "ideal" decoder at the receiver, which can always successfully decode the relevant signal. We do not consider a per BS sum-power constraint. Each BS emits with a sum-power which depends on the number of secondary users served by it.

The BS signals propagate through the wireless medium to reach the users. This process degrades the signal power of BS $\mathbf{z}_n$ received at the location of user $\mathbf{u}_i$, by a factor which depends on the distance $d(\mathbf{z}_n, \mathbf{u}_i)$ and by the power of a *complex valued* random fading component $e^{j\theta}\sqrt{g}$. The fading power is an independent realization of a unit-mean exponential random variable G and the phase is an independent realization of a uniform random variable Θ on $[0, 2\pi)$. We denote the total gain from the first (resp. second) neighbour $\mathbf{b}_{i1}$ ($\mathbf{b}_{i2}$) to user $\mathbf{u}_i$ by $h_{i1} := g_{i1} r_{i1}^{-\beta}$ ($h_{i2} := g_{i2} r_{i2}^{-\beta}$) and the total gain from the first (resp. second) neighbour $\mathbf{b}_{n1}$ ($\mathbf{b}_{n2}$) of some other user $\mathbf{u}_n$, to user $\mathbf{u}_i$ by $h_{n1,i} := g_{n1,i} d_{n1,i}^{-\beta}$ ($h_{n2,i} := g_{n2,i} d_{n2,i}^{-\beta}$), with $\beta > 2$. The related channel phases are θ_{i1} (θ_{i2}) and $\theta_{n1,i}$ ($\theta_{n2,i}$). The total signal received at user $\mathbf{u}_i$ is

$$\begin{aligned} y_i &= \left(s_i^{(pr)} + s_i^{(c1)}\right) e^{j\theta_{i1}} \sqrt{h_{i1}} + s_i^{(c2)} e^{j\theta_{i2}} \sqrt{h_{i2}} \\ &+ \sum_{\mathbf{u}_n \neq \mathbf{u}_i} f_n + \eta_i, \end{aligned} \quad (4)$$

where $f_n := \left(s_n^{(pr)} + s_n^{(c1)}\right) e^{j\theta_{n1,i}} \sqrt{h_{n1,i}} + s_n^{(c2)} e^{j\theta_{n2,i}} \sqrt{h_{n2,i}}$. The thermal noise is a realization of the r.v. $\eta_i \sim \mathcal{N}\left(0, \sigma_i^2\right)$, which follows the normal distribution. In the above the sum over $\mathbf{u}_n \neq \mathbf{u}_i$ is the interference received by user $\mathbf{u}_i$. The beneficial signal at the user location is equal to

$$\begin{aligned} &\mathcal{S}_i^{(\theta)}(a_i, p) = \\ &h_{i1}(1-a_i)\,p + h_{i2} a_i p + 2a_i p \sqrt{h_{i1} h_{i2}} \cos(\theta_{i1} - \theta_{i2}), \end{aligned} \quad (5)$$

and a similar term with the adequate indexing appears for each interference term due to user $\mathbf{u}_n \neq \mathbf{u}_i$. The term with the $\cos(\cdot)$ is an extra term which is related to the phases of the channels from the first and second neighbour and can be positive or negative depending on the phase difference. By controlling this term we can maximize the received beneficial signal. *If the phase θ_{i2} is known and communicated to the first neighbour*, the latter can choose to transmit with $\theta_{\mathbf{i1}} = \theta_{\mathbf{i2}}$. As a result the extra term is maximized, since $\cos(0) = 1$. The same action cannot be applied to the interference terms. The control affects only the primary user of each BS. The emitted signal for some user is interference for some other with a random fading phase in $[0, 2\pi)$. The expected value of the interference terms is $\mathbb{E}_\theta[\cos(\theta_{n1,i} - \theta_{n2,i})] = 0$ and the extra term disappears in expectation. Below, we will assume that the SINR takes the form

$$\mathrm{SINR}_i(\mathbf{a}, p) = \frac{\mathcal{S}_i(a_i, p)}{\sigma_i^2 + \mathcal{I}_i(\mathbf{a}_{-i}, p)} \quad (6)$$

$$\mathcal{S}_i(a_i, p) := h_{i1}(1-a_i)\,p + h_{i2} a_i p + 2a_i p \sqrt{h_{i1} h_{i2}} \quad (7)$$

$$\mathcal{I}_i(\mathbf{a}_{-i}, p) := \sum_{j \neq i} \mathcal{S}_{j,i}(a_j, p) \quad (8)$$

$$\mathcal{S}_{j,i}(a_j, p) := h_{j1,i}(1-a_j)\,p + h_{j2,i} a_j p. \quad (9)$$

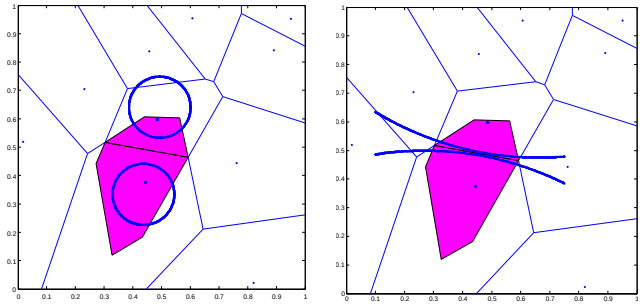

(a) Cooperation Regions $\rho = 0.4$. (b) Cooperation Regions $\rho = 0.9$

Fig. 3. Cooperation regions between two neighbouring BSs, in an example topology of 10 uniformly scattered atoms and two different values of ρ. (a) In the case of small ρ there can appear subregions of the 2-Voronoi cell where Full Coop can be applied, which lie away from the boundary and even "behind" the BS. (b) In the case of values of ρ close to 1 the Full Coop region tends to disappear, because the two circles reach the 1-Voronoi edge.

It will be shown in Section VI that this approximation, which considers the expectation of the interference term over $\theta_{n1,i},\ \theta_{n2,i}$ is justified for our model and produces results which are almost identical with the original one.

B. A Family of Geometric Policies: Full or No Cooperation

In all above SINR expressions, the vector of power-split-ratios $\mathbf{a}$ is not predifined and it gives a continuous range of cooperation possibilities. In this work we will focus on the two *user-optimal* cases $a_i = 0$ and $a_i = \frac{1}{2}$, given any fixed vector of choice $\mathbf{a}_{-i}$ for all users other than $\mathbf{u}_i$. To explain this choice, we show in the following that $a_i = 0$ and $a_i = \frac{1}{2}$ are the *two possible maximizers of the user signal power* $\mathcal{S}_i(a_i, p)$ in (7). We have

$$\frac{\partial \mathcal{S}_i(a_i,p)}{\partial a_i} = p\sqrt{h_{i1}h_{i2}}\left(-\sqrt{\frac{h_{i1}}{h_{i2}}}+\sqrt{\frac{h_{i2}}{h_{i1}}}+2\right) \quad (10)$$

Setting $\hat{\rho} = \sqrt{h_{i2}/h_{i1}}$, we solve the equation $-\hat{\rho}^{-1}+\hat{\rho}+2=0 \Rightarrow \hat{\rho}^2+2\hat{\rho}-1=0$ and find that, when $\hat{\rho} \geq 0.1716$, the derivative is non-negative and the optimal policy is $a_i^* = \frac{1}{2}$, so that full cooperation is optimal, otherwise no cooperation is optimal and $a_i^* = 0$. The optimal choice between the two values depends on the relative quality of the channel gains from the two neighbouring BSs, namely the ratio $\frac{h_{i2}}{h_{i1}}$. If we ignore (or average out) the random effects of the fast fading, the critical ratio is the distance ratio $\rho_i := \frac{r_{i1}}{r_{i2}}$. By substitution of the appropriate values of a_i in (6) we get:

- *No Cooperation* (No Coop) for $a_i = 0$, which gives

$$\mathrm{SINR}_i(0, \mathbf{a}_{-i}, p) = \frac{h_{i1}p}{\sigma_i^2 + \mathcal{I}_i(\mathbf{a}_{-i}, p)}. \quad (11)$$

- *Full Cooperation* (Full Coop) for $a_i = \frac{1}{2}$, which gives

$$\mathrm{SINR}_i\left(\frac{1}{2}, \mathbf{a}_{-i}, p\right) = \frac{\frac{\left(\sqrt{h_{i1}}+\sqrt{h_{i2}}\right)^2}{2}p}{\sigma_i^2 + \mathcal{I}_i(\mathbf{a}_{-i}, p)}. \quad (12)$$

Definition 1 *We will call user-optimal geometric policy with global parameter* $\rho \in [0,1]$*, the policy*

$$a_i = \begin{cases} 0 & \text{(No Coop)} \quad \text{, if } r_{i1} \leq \rho r_{i2} \\ \frac{1}{2} & \text{(Full Coop)} \quad \text{, if } r_{i1} > \rho r_{i2} \end{cases}. \quad (13)$$

This family of policies is *user-optimal* and *geometric* because the choice to cooperate or not depends only on the relative position of each user $\mathbf{u}_i$ to its two closest BSs. The ratio $\rho \in [0,1]$ defines the planar cooperation regions, has a global value for the network and is left as an optimization variable. Rather interestingly, the geometric locus of planar points with $r_{i1} \leq \rho r_{i2}$ for $\rho \in [0,1)$, where the policy chooses No Coop can easily be shown to be a *disc*. For $\rho = 1$ the locus degenerates to the line passing over the 1-Voronoi boundary of the two cells. The two extreme values of ρ give:
- Full Coop everywhere on the plane when $\rho = 0$.
- No Coop everywhere on the plane when $\rho = 1$.

Fig. 3(a) and Fig. 3(b) gives two examples for the geometric locus of points of Full Coop, given a realization of BS positions. The locus consists of all planar points for which $\mathbb{1}_{\{r_{i1}>\rho r_{i2}\ \&\ r_{i1}\leq r_{i2}\}} = \mathbb{1}_{\{r_{i1}>\rho r_{i2}\ \&\ \mathcal{V}_2(\mathbf{b}_{i1},\mathbf{b}_{i2})\}} = 1$, in other words the subregion of the 2-Voronoi cell which lies outside the No Coop discs. The larger the value of ρ, the "thinner" the cooperation region. In general, intermediate values of the cooperation paremeter, allow a combination of policies Full Coop and No Coop on the plane. In this way, a higher coverage benefit can be achieved, by serving points closer to base stations without cooperation and transmitting cooperatively for the points at the cell borders.

C. Relations between Willems' Encoding and Downlink MISO Beamforming

We shortly present here a different communication scheme, where beamformers are introduced in the CoMP model. In this scheme, the choice of different values for the beamformers, denoted by $w_{i1}, w_{i2} \in \mathbb{C}$, results in different expressions for the SINR. Depending on the amount of CSI available at the transmitter, we can reproduce the forms (5) and (12), and we derive the form of SINR when full CSI is available. In this setting no private/common splitting takes place and the user is served by exactly two BSs, transmitting the same signal, in which case $s_i = s_i^{(c)}$. Using the beamformers, the received signal is

$$\tilde{y}_i = \left(w_{i1}e^{j\theta_{i1}}\sqrt{h_{i1}} + w_{i2}e^{j\theta_{i2}}\sqrt{h_{i2}}\right)s_i + \sum_{\mathbf{u}_n \neq \mathbf{u}_i} \tilde{f}_n + \eta_i, \quad (14)$$

where $\tilde{f}_n = \left(w_{n1}e^{j\theta_{n1,i}}\sqrt{h_{n1,i}} + w_{n2}e^{j\theta_{n2,i}}\sqrt{h_{n2,i}}\right)s_n$. The beamformers are related through the equality $|w_{i1}|^2+|w_{i2}|^2 = 1$. Here we differentiate between cases having different CSI.

• **Case 1** No CSI available: $w_{i1}, w_{i2} \in \mathbb{R}$ and $w_{i1} = w_{i2} = 1/\sqrt{2}$.

$$\tilde{\mathcal{S}}_i\left(1/\sqrt{2}, 1/\sqrt{2}, p\right) = \frac{1}{2}h_{i1}p + \frac{1}{2}h_{i2}p + p\sqrt{h_{i1}h_{i2}}\cos(\theta_{i1}-\theta_{i2}). \quad (15)$$

This form reproduces (5) with $a_i = 1/2$.

• **Case 2** Partial CSI available, only channel phase: $w_{i1}, w_{i2} \in \mathbb{C}$ and $w_{i1} = e^{-j\theta_{i1}}/\sqrt{2}$, $w_{i2} = e^{-j\theta_{i2}}/\sqrt{2}$.

$$\tilde{\mathcal{S}}_i\left(e^{-j\theta_{i1}}/\sqrt{2}, e^{-j\theta_{i2}}/\sqrt{2}, p\right) = \frac{1}{2}h_{i1}p + \frac{1}{2}h_{i2}p + p\sqrt{h_{i1}h_{i2}}. \quad (16)$$

This form reproduces the signal in (12). It is often referred to as *Equal Gain Combining*.

• **Case 3** Full CSI available: $w_{i1}, w_{i2} \in \mathbb{C}$ and $w_{i1} = \frac{\sqrt{h_{i1}}}{\sqrt{h_{i1}+h_{i2}}}e^{-j\theta_{i1}}$, $w_{i2} = \frac{\sqrt{h_{i2}}}{\sqrt{h_{i1}+h_{i2}}}e^{-j\theta_{i2}}$.

$$\tilde{\mathcal{S}}_i\left(\frac{\sqrt{h_{i1}}}{\sqrt{h_{i1}+h_{i2}}}e^{-j\theta_{i1}}, \frac{\sqrt{h_{i2}}}{\sqrt{h_{i1}+h_{i2}}}e^{-j\theta_{i1}}, p\right) = p\left(h_{i1}+h_{i2}\right). \quad (17)$$

Obviously (15)≤(16)≤(17).

Although the SINR formulas of Willems' encoding can be reproduced by beamforming in a straightforward manner, they merit great interest due to the possibility to optimally shift between No Coop and Full Coop depending on the relative channels. In other words the power-split-ratio a_i adapts the scheme better to the actual channel conditions.

III. Stochastic Geometry and Coverage

We can now formulate the problem within the framework of Stochastic Geometry [29]. We focus on a typical location on the plane and since we deal with translation invariant models, we can set its coordinates as the origin $(0,0)$ without loss of generality. We assume that a user is positioned at this point, whom we denote by $\mathbf{u}_o$. The two closest BSs are $\mathbf{b}_1 := \mathbf{b}_{o1}$, $\mathbf{b}_2 := \mathbf{b}_{o2}$ with distances $r_1 = r_{o1}$, $r_2 := r_{o2}$ from the typical location. The channel gains are further defined as $h_1 := h_{o1} = g_1 r_1^{-\beta}$, $h_2 := h_{o2} = g_2 r_2^{-\beta}$, $h_{n1} := h_{n1,o} = g_{n1} d_{n1}^{-\beta}$ and $h_{n2} := h_{n2,o} = g_{n2} d_{n2}^{-\beta}$. Furthermore, g_1, g_2, g_{n1} and g_{n2} are realizations of independent exponential r.v.'s with mean p (the individual per-user power) $G_{ni}, G_i \sim \exp(1/p)$, $i = 1, 2$. Consequently, $\sqrt{G}$ follows the Rayleigh distribution. The aim of this section is to derive the coverage probability of the cooperation scheme:

$$q_c(T, \lambda, \beta, p, \rho) := \mathbb{P}\left[\mathrm{SINR} > T\right], \quad (20)$$

Notice that it would be more natural to consider the SINR at the location of a *typical user* and that the two definitions do not coincide here because the point process of BSs and that of users are not independent. The *typical location* refers to a typical 2D planar point and follows the standard approach used to analyze stationary and homogeneous point processes (p.p.'s), by evaluating the system performance at just one representative planar point, chosen at the Cartesian origin [30], as in [16] and [17]. The performance at any other planar point will exhibit the same behaviour. However, we cannot use in our paper the notion of a *typical user* interchangeably with that of *typical location*, because of the modelling assumption of 1 user per 1-Voronoi cell. The resulting set of users is a different non-Poisson p.p., where the density of users in 1-Voronoi cells with small surface is greater than in those with larger surface. For the *typical user* in our model, it would not be possible to use Slivnyak's theorem and the results for PPPs that we have below.

The coverage probability is a function of the threshold T, the PPP intensity λ, the pathloss exponent β, the user power p and the policy parameter ρ. From here on, the parameter set $\{T, \lambda, \beta, p\}$, which does not influence the analysis, is omitted from the arguments. The SINR for the typical location can now be written as in (18), using the policies in Definition 1 and the expressions (11) and (12). The interference $\mathcal{I}(\rho, r_2)$ takes into consideration all the power splitting decisions of primary users related to BSs with distance $d_{n1}, d_{n2} \geq r_2$ from the origin - the reader can refer to (8). The decisions are globally determined by the value of ρ.

A. Distribution of distance to the two closest neighbours

For the stochastic geometry analysis, we will need the following two results related to the distance distribution.

Lemma 1 *Given a PPP of intensity λ, the joint p.d.f. of the distances (r_1, r_2) between the typical location $\mathbf{u}_o$ and its first and second closest neighbour, is equal to*

$$f_{r_1,r_2}(r_1, r_2) = (2\lambda\pi)^2 r_1 r_2 e^{-\lambda\pi r_2^2}. \quad (21)$$

The expected value of the distance r_2 is equal to $\mathbb{E}[r_2] = \frac{3}{4\sqrt{\lambda}} \geq \mathbb{E}[r_1] = \frac{1}{2\sqrt{\lambda}}$.

Proof: To determine the first closest neighbour, we should find the largest ball $\mathcal{B}(\mathbf{u}_o, r_1)$ of radius r_1 which is empty. This ball meets the first neighbour on its boundary and since the interior of the ball is empty of atoms, the location belongs to the 1-Voronoi cell (1) of this atom. We further enlarge the ball until the second closest neighbour is met on the boundary of $\mathcal{B}(\mathbf{u}_o, r_2)$, $r_2 > r_1$ and the first (and no other) is contained in its interior. The case of two atoms lying on the boundary has zero probability as a property of the PPP [29]. Consequently, the typical location belongs to the 2-Voronoi cell (2) of these two BSs. In this way, the annulus starting from the ball of radius r_1 and reaching the ball of radius r_2 is the largest empty.

We denote by s and t the stopping times for hitting the first and second neighbour respectively. The tail distribution of t, given s, is equal to

$$\mathbb{P}\left[t > r_2 | s = r_1,\ r_2 \geq r_1\right] = \mathbb{P}\left[\phi\left(\mathbf{int}\left(\mathcal{B}(\mathbf{u}_o, r_1) \cap \mathcal{B}(\mathbf{u}_o, r_2)\right)\right) = 0\right] = e^{-\lambda\pi\left(r_2^2 - r_1^2\right)}.$$

This results in,

$$f_{r_2|r_1}(r_2|r_1) = 2\lambda\pi r_2 e^{-\lambda\pi\left(r_2^2 - r_1^2\right)}$$

and using Bayes' rule for p.d.f.'s

$$f_{r_1,r_2}(r_1, r_2) = f_{r_2|r_1}(r_2|r_1) \cdot f_{r_1}(r_1) = (2\lambda\pi)^2 r_1 r_2 e^{-\lambda\pi r_2^2}.$$

Using this, we can calculate the expected value of r_2

$$\mathbb{E}[r_2] = \int_0^\infty r_2 \int_0^{r_2} (2\lambda\pi)^2 r_1 r_2 e^{-\lambda\pi r_2^2}\, \mathrm{d}r_1\, \mathrm{d}r_2 = \int_0^\infty r_2 (2\lambda\pi)^2 \frac{r_2^3}{2} e^{-\lambda\pi r_2^2}\, \mathrm{d}r_2 = \frac{3}{4\sqrt{\lambda}}.$$

■

$$\mathrm{SINR}\left(\rho, r_1, r_2\right) = \frac{g_1 r_1^{-\beta}}{\sigma^2 + \mathcal{I}\left(\rho, r_2\right)} \mathbb{1}_{\{r_1 \le \rho r_2\}} + \frac{\frac{\left(\sqrt{g_1 r_1^{-\beta}} + \sqrt{g_2 r_2^{-\beta}}\right)^2}{2}}{\sigma^2 + \mathcal{I}\left(\rho, r_2\right)} \mathbb{1}_{\{r_1 > \rho r_2 \ \& \ r_1 \le r_2\}}, \tag{18}$$

$$\mathcal{L}_Z\left(s, \mu_1, \mu_2\right) = \frac{-s\sqrt{\frac{1}{\mu_1\mu_2}}\pi + s\sqrt{\frac{1}{\mu_1\mu_2}} \arctan\left(\sqrt{\frac{\mu_1}{\mu_2}} g\left(s\right)\right) + s\sqrt{\frac{1}{\mu_1\mu_2}} \arctan\left(\sqrt{\frac{\mu_2}{\mu_1}} g\left(s\right)\right) + g\left(s\right)}{g\left(s\right)^3}, \tag{19}$$

An important lemma below, provides the expression for the probability for a user not to ask for cooperation, based on the region $r_1 \le \rho r_2$. The interesting observation is that the parameter $\rho \in [0,1]$ fully determines this probability.

Lemma 2 *The probability of a user not to demand for BS cooperation for its service is*

$$\mathbb{P}\left[\text{No Coop}\right] = \mathbb{P}\left[r_1 \le \rho r_2\right] = \rho^2. \tag{22}$$

Proof: We make use of the expression for the joint p.d.f. of the pair of distances (r_1, r_2) in (21) of Lemma 1. Then the probability $\mathbb{P}\left[r_1 \le \rho r_2\right]$ is calculated by the double integral

$$\begin{aligned}
\mathbb{P}\left[r_1 \le \rho r_2\right] &= \int_0^\infty \int_{r_1}^\infty \mathbb{1}_{\{r_1 \le \rho r_2\}} \left(2\lambda\pi\right)^2 r_1 r_2 e^{-\lambda\pi r_2^2} \, \mathrm{d}r_2 \, \mathrm{d}r_1 \\
&= \int_0^\infty \int_{\frac{r_1}{\rho}}^\infty \left(2\lambda\pi\right)^2 r_1 r_2 e^{-\lambda\pi r_2^2} \, \mathrm{d}r_2 \, \mathrm{d}r_1 \\
&= \int_0^\infty 2\lambda\pi r_1 e^{-\lambda\pi\left(\frac{r_1}{\rho}\right)^2} \, \mathrm{d}r_1 = \rho^2.
\end{aligned}$$

■

B. Cooperative Channel Fading Distribution and Properties

In this subsection we derive a general expression for the distribution of the signal power when full cooperation is applied. Furthermore, certain properties of this distribution are provided.

Lemma 3 *Given the r.v.'s $G_i \sim \exp\left(1/p_i\right)$, $i = 1, 2$, the Laplace Transform (LT) of the r.v.*

$$Z_{r_1, r_2} := \left(\sqrt{G_1 r_1^{-\beta}} + \sqrt{G_2 r_2^{-\beta}}\right)^2 \tag{23}$$

is equal to (19), where $g\left(s\right) := \sqrt{1 + \left(\frac{1}{\mu_1} + \frac{1}{\mu_2}\right) s}$ and $\mu_i := \frac{r_i^\beta}{p_i}$ for $i = 1, 2$. Furthermore, its p.d.f. is square integrable and its expectation is equal to

$$\mathbb{E}\left[Z_{r_1, r_2}\right] = \sqrt{\frac{1}{\mu_1\mu_2}} \left(\frac{\pi}{2} + \frac{\mu_1 + \mu_2}{\sqrt{\mu_1\mu_2}}\right). \tag{24}$$

Proof: See Appendix B. ■

We further provide an interesting property of the r.v. $\frac{Z_{r,r}}{2}$ of the fading for Full Coop, in the special case of $\mu_1 = \mu_2 = \mu := \frac{r^\beta}{p}$ (the expression given in (23)), with relation to the r.v. $G \sim \exp\left(\mu\right)$, which is the case for No Coop. We use the notion of the *Laplace-Stieltjes transform ordering* [31] based on which, the r.v. Y dominates the r.v. X and we write $X \le_L Y$, if $\mathcal{L}_X\left(s\right) \ge \mathcal{L}_Y\left(s\right)$, for all $s \ge 0$.

Lemma 4 *Given $\mu_1 = \mu_2 = \mu := \frac{r^\beta}{p}$, and the two r.v.'s $G \sim \exp\left(\mu\right)$ and $Z_{r,r}/2$ from (23), the following Laplace-Stieltjes transform ordering inequality holds*

$$G \le_L \frac{Z_{r,r}}{2}. \tag{25}$$

Proof: We first establish a simple result. It can be easily shown that for the p.d.f. $f_{\frac{Z}{2}}\left(t\right) = 2 f_Z\left(2t\right)$. Taking the Laplace transform and using the above equality for the p.d.f.'s we get $\mathcal{L}_{\frac{Z}{2}}\left(s\right) = \mathbb{E}_{\frac{Z}{2}}\left[e^{-st}\right] = \mathbb{E}_Z\left[e^{-\frac{s}{2}2t}\right] = \mathcal{L}_Z\left(\frac{s}{2}\right)$. The LT of the r.v. G is equal to

$$\mathcal{L}_G\left(s\right) = \frac{1}{1 + sp},$$

while the LT of the r.v. $\frac{Z_{r,r}}{2}$ is found using the above observation and the form in (19)

$$\begin{aligned}
\mathcal{L}_{Z_{r,r}/2}\left(s\right) &= \mathcal{L}_Z\left(\frac{s}{2}, \mu, \mu\right) \\
&= \frac{1}{1 + sp}\left(1 + sp\frac{-\pi/2 + \arctan\left(\sqrt{1 + sp}\right)}{\sqrt{1 + sp}}\right).
\end{aligned}$$

The range of $\arctan\left(\sqrt{1 + sp}\right) \in [\pi/4, \pi/2]$ and hence the term in the parenthesis is $(\cdot) \le 1$. ■

Under the constraint that $\mu < 1$, a similar inequality can be proven by using the notion of *stochastic ordering* [32, A4. p.411]. The r.v. Y stochastically dominates the r.v. X and we write $X \le_{st} Y$, if $\mathbb{P}\left[X > t\right] \le \mathbb{P}\left[Y > t\right]$ for all t.

C. Interference as Shot Noise

In the current subsection, we describe the interference $\mathcal{I}\left(\rho, r_2\right)$ as a shot-noise field [29, Ch.2] generated by a point process outside a ball of radius r_2. Following Definition 1, we consider all the power splitting decisions of primary users $\mathbf{u}_j$ (either $a_j = 0$ or $a_j = 1/2$) related to BSs with distance $d_{j1} \ge r_2$ from the origin. The decisions are determined by the value of the global parameter ρ of the geometric policies. By substitution of these two values for the power-split-ratio in (8) and (9), the interference received at $\mathbf{u}_o$ is equal to

$$\mathcal{I}\left(\rho, r_2\right) = \sum_{\mathbf{u}_n \ne \mathbf{u}_o} h_{n1} \mathbb{1}_{\{r_{n1} \le \rho r_{n2}\}} + \frac{h_{n1} + h_{n2}}{2} \mathbb{1}_{\{r_{n2} \ge r_{n1} > \rho r_{n2}\}}.$$

The geometry is illustrated in Fig. 4. To derive a more tractable expression for the interference, which takes into

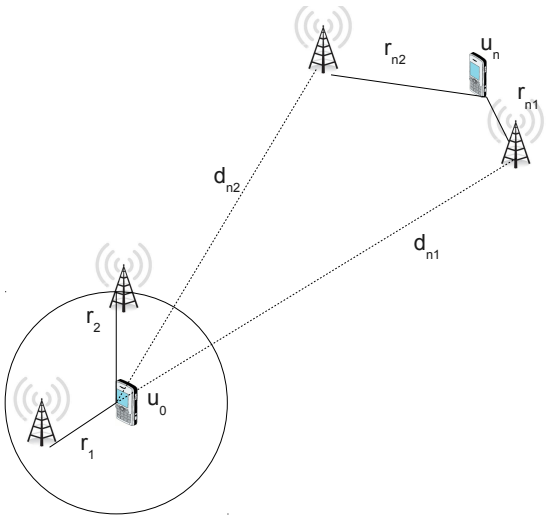

Fig. 4. Illustration of the interference model with a single interfering pair lying outside the ball of radius r_2.

account the random positioning of the users, suppose that each atom $\mathbf{z}_n$ of the BS point process has a primary user $\mathbf{u}_n$ who, with probability $\mathbb{P}[r_{n1} \leq \rho r_{n2}]$ lies within the No Coop region. From Lemma 2 this probability is equal to ρ^2, whereas with probability $1-\rho^2$ the user requests for Full Coop. Then we consider that each BS is associated with a *binary* r.v. $B_n \sim \text{Bernoulli}(\rho^2)$ such that

$$B_n \quad = \quad \begin{cases} 1 & \text{with prob. } \rho^2 \quad \text{(No Coop)} \\ 0 & \text{with prob. } 1-\rho^2 \quad \text{(Full Coop)} \end{cases} . \quad (26)$$

Each BS is related to an independent B_n. Then:

- If $B_n = 1$, an independent mark $\mathcal{M}_n$ is associated with the BS. The mark is equal to $\mathcal{M}_n := d_n^{-\beta} G_n$, and this signal is treated as interference at the typical location, where $G_n \sim \exp(1/p)$. The signal has to traverse a distance of $d_n = d_{n1}$ from the closest neighbour of user $\mathbf{u}_n$, as shown in Fig. 4.
- If $B_n = 0$, an independent mark $\mathcal{N}_n$ is associated with the BS. This is the case of Full Coop, where the interfering signal due to user $\mathbf{u}_n$ is jointly emitted from its two closest neighbours. Here, we make the *far-field approximation* $d_{n1} \approx d_{n2} = d_n$, where the distances of the two cooperating atoms to the typical location are treated as equal. Such a heuristic is allowed, since the two closest neighbours of user $\mathbf{u}_n$ are expected to lie close to each other and at the same time, outside of the ball of radius r_2. In this sense we can expect that the error is small. Based on this approximation, BSs with primary users requiring Full Coop, are considered to emit the entire signal $\mathcal{N}_n := d_n^{-\beta} \frac{G_{n1}+G_{n2}}{2}$, $G_{n1}, G_{n2} \sim \exp(1/p)$.

This heuristic representation of the interference will be referred to as the *far-field approximation*. It is interesting to notice that, the r.v. G_n, related to the mark $\mathcal{M}_n$ follows the exponential distribution, or equivalently the $\Gamma(1,p)$ distribution, with expected value p, whereas the r.v. $\frac{G_{n1}+G_{n2}}{2}$ related to $\mathcal{N}_n$, follows the $\Gamma\left(2, \frac{p}{2}\right)$, with the same expected value p. In other words, the path-loss of the interfering signals is in expectation equal in both cases (of either Full Coop or No Coop for the interfering user). In this far-field approximation, the interference random variable can be expressed as

$$\mathcal{I}(\rho, r_2) := r_2^{-\beta} G_2 B_2 + r_2^{-\beta} \frac{G_1+G_2}{2}(1-B_2) + \sum_{\mathbf{z}_n \in \phi \setminus \{\mathbf{b}_1, \mathbf{b}_2\}} d_n^{-\beta} G_n B_n + d_n^{-\beta} \frac{G_{n1}+G_{n2}}{2}(1-B_n), \quad (27)$$

where the first two terms come from the interference created by the second neighbour lying on the boundary of the ball $\mathcal{B}(\mathbf{u}_o, r_2)$. Finally we derive the LT $\mathcal{L}_{\mathcal{I}}(s, \rho, r_2)$ of the Interference variable.

We are now ready to present our first important result, which is the LT of the interference. For its proof, we make use of Lemma 2 and the discussion above. The novelties in the result and the proof are related to the way we handle the interference field as a summation of two independent point processes, one whose BSs cooperate and one who do not. Their union is obviously the union of points of the original PPP with distance $\geq r_2$. Another new concept is that the position of the closest (and strongest) interferer coincides with the radius of the second neighbour, which is known. This creates an extra term at r_2 to be considered in the sum.

Theorem 1 *For Rayleigh fading, the LT of the far-field approximation Interference is equal to*

$$\mathcal{L}_{\mathcal{I}}(s, \rho, r_2) = \mathcal{L}_{\mathcal{J}}(s, \rho, r_2)\, e^{-2\pi\lambda \int_{r_2}^{\infty} (1 - \mathcal{L}_{\mathcal{J}}(s,\rho,r)) r \, \mathrm{d}r}, \quad (28)$$

where

$$\mathcal{L}_{\mathcal{J}}(s, \rho, r) = \rho^2 \frac{1}{1+sr^{-\beta}p} + \left(1-\rho^2\right) \frac{1}{\left(1+sr^{-\beta}\frac{p}{2}\right)^2}. \quad (29)$$

Proof: See Appendix C. ∎

It can be shown that the LT of the interference r.v. $\mathcal{L}_{\mathcal{I}}(s, \rho, r_2)$ in (28) is a non-decreasing function in ρ and r_2 and non-increasing function in s. A direct consequence of this is that the LT of the interference takes its maximal value for $\rho = 1$. This is based on the Laplace-Stieltjes transform ordering. The argument is that for any $0 \leq \rho_a < \rho_b \leq 1$, $\mathcal{L}_{\mathcal{I}}(s, \rho_a, r_2) \leq \mathcal{L}_{\mathcal{I}}(s, \rho_b, r_2) \Rightarrow \mathcal{I}(\rho_a, r_2) \geq_L \mathcal{I}(\rho_b, r_2) \geq_L \mathcal{I}(1, r_2)$. The larger ρ the smaller the interference. Similarly, the larger the distance to the second neighbour r_2, the smaller the interference, because a larger empty ball of interferers around the typical location is guaranteed. Finally, we give the expression of the expected value for the Interference r.v.

$$\mathbb{E}[\mathcal{I}(\rho, r_2, \beta, p, \lambda)] = \frac{p}{(\beta-2) r_2^{\beta}} \left(\beta - 2 + 2\pi\lambda r_2^2\right). \quad (30)$$

The expected value of the interference r.v. is *independent of the parameter* ρ. This means that all scenarios of cooperation for any $\rho \in [0,1]$ are compared to each other, with reference to an interference field with the same expected value (30). Observe that $\lim_{r_2 \to 0} \mathbb{E}[\mathcal{I}(\rho, r_2, \beta, p, \lambda)] = \infty$, for $\beta > 2$ and irrespective of the power p.

$$q_c(\rho) = \int_0^\infty \int_{\frac{r_1}{\rho}}^\infty (2\lambda\pi)^2 r_1 r_2 e^{-\lambda\pi r_2^2} \cdot e^{-\frac{r_1^\beta}{p} T\sigma^2} \mathcal{L}_{\mathcal{I}}\left(\frac{r_1^\beta}{p} T, \rho, r_2\right) \mathrm{d}r_2\, \mathrm{d}r_1 + \\ + \int_0^\infty \int_{r_1}^{\frac{r_1}{\rho}} (2\lambda\pi)^2 r_1 r_2 e^{-\lambda\pi r_2^2} \int_{-\infty}^\infty e^{-2j\pi\sigma^2 s} \mathcal{L}_{\mathcal{I}}(2j\pi s, \rho, r_2) \frac{\mathcal{L}_Z\left(-j\pi s/T, \frac{r_1^\beta}{p}, \frac{r_2^\beta}{p}\right) - 1}{2j\pi s} \mathrm{d}s\, \mathrm{d}r_2\, \mathrm{d}r_1. \quad (31)$$

D. General Coverage Probability

In the current subsection we derive the coverage probability expression for the model under study with the far-field approximation of the interference field. For the proof of the Theorem that follows we make use of the results for the distribution of the distance of the two closest BSs in Lemma 1, the LT of the cooperation signal Z in Lemma 3, as well as the LT of Interference in Theorem 1.

Theorem 2 *For the cooperation scenario under study and for a given set of system values $\{T, \lambda, \beta, P\}$, the coverage probability at the typical location as a function of the parameter $\rho \in [0,1]$ is equal to $q_c(\rho) = q_{c,1}(\rho) + q_{c,2}(\rho)$, and is given in (31).*

In this expression, $\mathcal{L}_{\mathcal{I}}(s, \rho, r_2)$ is the LT of $\mathcal{I}$ given in (28), (29) and $\mathcal{L}_Z(s, \mu_1, \mu_2)$ is the LT of the general fading r.v. Z_{r_1,r_2} given in (19).

Proof: See Appendix C. ∎

Using this formula, we can numerically evaluate the coverage probability of any system with pairwise cooperation and Full/No Coop policies. Furthermore, the use of Laplace Transforms has facilitated the comprehension of the system model and has provided more intuition. To see why, we refer the reader to the expressions which show the expected values for the signal and the interference, in formulas (24), (30) and later (34), as well as Lemma 4, and the monotonicity results under Theorem 1.

IV. Second Neighbour Interference Elimination - Dirty Paper Coding (DPC)

The first and second geographic BS neighbour are the most influential on the interference power, due to their proximity to the typical location. In this section we consider an ideal scenario, where the possible interference created by the two closest BS are cancelled out perfectly in the case of full cooperation, by means of coding. This requires that the first neighbour has precise *knowledge* of the interfering signal from the primary user of $\mathbf{b}_2$, as well as all possible secondary users served by $\mathbf{b}_1$ and $\mathbf{b}_2$. This is extra information for the system. If such information is available, the encoding procedure for the signal related to the typical location can be projected on the orthogonal signal space of the interfering signals, achievable by Dirty Paper Coding, so that the effect of $\mathbf{b}_1$ and $\mathbf{b}_2$ on interference is eliminated (see [33] - however notice that we do not refer here to the Zero Forcing and Dirty Paper coding scheme in [34] because such a scheme would require full channel state information feedback). If the elimination is perfect, the SINR for the typical location should be rewritten as in (18), where the interference in the case of full cooperation has been replaced by the r.v. $\mathcal{I}_{DPC}$.

$$\mathcal{I}_{DPC}(\rho, r_2) = \\ \sum_{\mathbf{z}_n \in \phi \setminus \{\mathbf{b}_1, \mathbf{b}_2\}} d_n^{-\beta} G_n B_n + d_n^{-\beta} \frac{G_{n1} + G_{n2}}{2} (1 - B_n), \quad (32)$$

and its Laplace Transform

$$\mathcal{L}_{\mathcal{I}_{DPC}}(s, \rho, r_2) = e^{-2\pi\lambda \int_{r_2}^\infty (1 - \mathcal{L}_{\mathcal{J}}(s,\rho,r)) r\, \mathrm{d}r}, \quad (33)$$

where $\mathcal{L}_{\mathcal{J}}(s, \rho, r)$ is given in (29). Notice that if the user chooses No Coop, the elimination is not possible. The expected value of the interference without the influence of $\mathbf{b}_2$ is smaller than the expression in (30) by $\frac{\beta - 2 + 2\pi\lambda r_2^2}{2\pi\lambda r_2^2} > 1$, $\beta > 2$, as the following formula shows

$$\mathbb{E}\left[\mathcal{I}_{DPC}(\rho, r_2, \beta, p, \lambda)\right] = \frac{p}{(\beta - 2) r_2^\beta} 2\pi\lambda r_2^2. \quad (34)$$

The expected value of DPC interference is independent of the cooperation parameter ρ. In Theorem 2 and the expression for coverage probability in (31), the LT $\mathcal{L}_{\mathcal{I}}$ should be replaced by $\mathcal{L}_{\mathcal{I}_{DPC}}$ (33), only at the cooperation part (i.e. the second integral).

V. Pros and Cons of BS-Pair Conferencing

The coverage probability expression in (31) can provide intuition on the change in coverage probability when applying different ρ-cooperation policies.

Pros: The gains of the cooperation scheme result from three reasons.

- The specific coding scheme enabled by conferencing provides an extra term of $2a_i p\sqrt{h_{i1}h_{i2}} \overset{a_i=1/2}{=} p\sqrt{h_{i1}h_{i2}}$ for the beneficial signal in (7). Given that the channel fast fading r.v.'s follow an exponential distribution, for the symmetric case $r_1 = r_2 = r$, the resulting Full Coop variable $Z_{r,r}/2$ is larger than G in the Laplace ordering sense, as shown in Lemma 4. From an engineering perspective, the user transmission power is equally divided between the two closest BS neighbours, who transmit the same signal with power $p/2$. Since the signals add-up coherently at the receiver at the typical location, this can provide an increase in the received signal power, but depends also on the distances of the two BSs from the user.
- The knowledge of the second closest neighbour exact position (related to the typical location), guarantees an open ball of radius $r_2 > r_1$ to be interference free. The expected radius $\mathbb{E}[r_2] = \frac{3}{4\sqrt{\lambda}}$ is strictly larger than $\mathbb{E}[r_1] = \frac{1}{2\sqrt{\lambda}}$. This means that there will be a factor of improvement on interference, compared to the case of no cooperation.

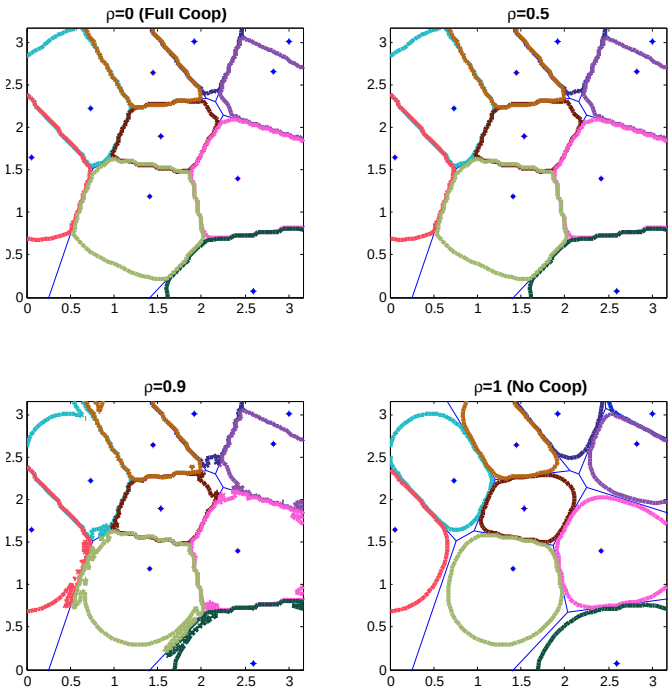

Fig. 5. Illustration of how the coverage regions are modified with variations of the value of the parameter ρ for a single realisation of the PPP in a window of size ($3.33m \times 3.33m = 10m^2$) and threshold value $T = 0.8$. We consider the case without fading to obtain smooth contours. For the chosen value of T, numerical evaluation (and also the relevant plots) show that the maximum coverage is achieved in the case of $\rho^* = 0.5$ (optimal). Numerically, the coverage difference with the case of Full Coop (everywhere) for $\rho = 0$ is just a bit smaller. For these two values, it can be seen that most areas at the cell edges are covered, whereas the case of No Coop with $\rho = 1$ fails to do so. As our policy dictates, when $\rho = 0.5$, only a part of the cell is served by cooperation and its complement without cooperation. To conclude, the benefits of the cooperation scheme can be maximised when cells are split in two areas, one near the centre where No Coop is applied and one at the cell boundary where Full Coop is applied.

• Cooperation is in favour of the cell-edge areas and offers coverage, when No Coop fails to do so. In Fig. 5 we illustrate the coverage areas for an instance of BS positions and when no channel fading is taken into account (so that smooth contours are visible). Observe the obvious increase of the coverage lobe in all cells when ρ decreases from 1 and reaches an optimum when $\rho = 0.5$. For this value, a part of the cell near the borders is treated with Full Coop and the other part near the centre is treated with No Coop. Hence, a change of the parameter ρ results in a change of the shape, so that certain planar points not covered when $\rho = 1$ can be covered for some other value $\rho < 1$. The parameter ρ can be chosen optimally as ρ^* (in our example 0.5), so that the geometric policy maximizes coverage. The optimal value of ρ depends on the set of model parameters (T, λ, β, p). The expression in (31) cannot be shown to be concave in ρ, and the existence of local optima cannot be excluded. The global optimum is found numerically. To summarize, it is important to keep in mind that it is often optimal with respect to coverage to split the cell in zones of Full Coop and No Coop, rather than apply Full Coop everywhere.

Cons: The negative effects of the cooperation scheme result from three reasons.

• The fair model we have introduced to evaluate the performance of pairwise cooperation in cellular networks will serve exactly 1 user per 1-Voronoi cell. In the case of cooperation with some parameter ρ, the users inside the cooperation zone will be served by the BS in their own cell as well as their 2nd closest neighbour. The latter could be one of the two BSs serving the typical location, thus creating first-order interference, which is very severe. For this reason, the performance of the scheme can be poor as will be shown in the plots later. Especially for higher thresholds T the Full Coop scheme may be inferior to No Coop. Lifting this interference by use of DPC is one solution we propose here, that improves the performance of cooperation.

• The parameter ρ of the geometric policy may force a user at a planar point $\mathbf{z}$ to ask for cooperation, even when $g_1 r_1^{-\beta} > \frac{\left(\sqrt{g_1 r_1^{-\beta}} + \sqrt{g_2 r_2^{-\beta}}\right)^2}{2}$. The reason is that geometric policies do not adapt to the actual fast-fading realization and depend only on the ratio $\frac{r_1}{r_2}$. Since ρ is a design parameter, the optimal ρ^* is expected to adapt, up to a certain degree, the policy to such events.

• By comparing the tail probabilities of $\frac{Z_{r_1,r_2}}{2}$ and the exponential No Coop signal G, we can find many examples of pairs (r_1, r_2), such that there exist values of the signal threshold T above which $\mathbb{P}[Z_{r_1,r_2}/2 > T] < \mathbb{P}[G > T]$. Above a certain threshold, the contribution of the exponential No Coop signal power to the coverage probability may be more considerable than the Full Coop signal power. As a consequence, there are values of the threshold T, above which the coverage probability of the No Coop everywhere scheme is optimal and cooperation turns out to be suboptimal.

VI. Numerical Evaluation and Simulations

The coverage probability given in Theorem 2 as a sum of the two integrals in (31) can be numerically evaluated using MATLAB. We use routines for single and double integrals (quad, quadgk and dblquad) to evaluate the triple and quadruple integrals by nested integration.

To guarantee the validity of the analysis and of the derived results, we have further developed a simulator, which builds a PPP of intensity $\lambda_{sim} = 1$ atom/m^2 for the positions of the BSs, within a finite square observation window of surface $W = 20$ m^2 (size of the x axis $\sqrt{20}$ m). For each realization, a Poisson generator produces a random number of atoms N with expected value $\mathbb{E}[N] = \lambda_{sim} W = 20$ atoms, which are further positioned uniformly over the square. This configuration of points coincides with the distribution of points of the PPP on a bounded window as shown in [29, pp.14-15]. The approximations and analytical evaluation of the integrals are validated by these simulations. A total number of ten thousand uniformly drawn scenarios is averaged to derive the estimation on the simulated coverage probability. The curves that appear in all coverage plots are related to the three cases of Full Coop everywhere ($\rho = 0$), No Coop everywhere ($\rho = 1$) and Optimal Coop, where the cell is optimally split by the parameter $\rho^* \in [0, 1]$, into a region close to the BS with No Coop and another one close to the boundary, with Full Coop. The optimal ρ^* is the one maximising coverage,

given different system parameters. Observe that the coverage probability results are independent of the BS density in the case of noiseless channel and SIR. For cases with noise, an appropriate modification of the noise variance gives the same curves.

A. Evaluation of model approximations (θ-related SINR and far-field approximation)

In Fig. 6(a) the coverage probability curves using two different SINR models are presented and compared. The first one, refers to the SINR in (6)-(9) with $\cos(\theta_{n1,i} - \theta_{n2,i})$ replaced by $\mathbb{E}_\theta[\cos(\theta_{n1,i} - \theta_{n2,i})] = 0$ at the interference. The second refers to the SINR without taking the expectation, but rather randomly picking $\theta_{n1,i}, \theta_{n2,i} \in [0, 2\pi]$ and including $\cos(\theta_{n1,i} - \theta_{n2,i})$ at the interference terms, as in (5). The curves are produced by the simulator. It is evident from the curves that for the range of parameters of interest here, the two models produce almost identical results and hence the approximation is valid. Intuitively, in each single realization of the PPP the $\cos(.)$ is randomly positive or negative for each BS n and can either add or remove to the interference.

In Fig. 6(b), we numerically evaluate, for $\beta = 4$, the difference between coverage curves with and without the far-field approximation (Fig. 4), in order to assess the validity of its approximation. Before discussing the figures, we should note that the approximation is reasonable for pairs of atoms that are far enough from the typical location, but becomes problematic for pairs in which the distance between atoms is comparable with that from the origin. Going now to the figure, it can be observed that although the curve for No Coop is almost the same with and without the approximation, this does not hold for the Full and Optimal Coop simulation curves. The coverage probability deteriorates faster than the analytical results for higher thresholds, which suggests that the approximation underestimates the effect of interference. The main reason is that, when considering the actual model with $d_{n1} \neq d_{n2}$ for some user $\mathbf{u}_n \neq (0, 0)$, *this user may be served as secondary by the first BS closest to the typical location, i.e.* $\mathbf{b}_1$. In such a case, its signal creates the highest possible interference, since it stems from the closest possible distance. This effect is however not apparent when DPC is applied, since all interference created from the cooperating pair to the typical location is diminished.

B. Coverage $q(\rho)$ Versus Threshold T, $\beta = 4$

In the plots of Fig. 7(a), the coverage probability is plotted with respect to the threshold value T, given the model approximations evaluated in the previous subsection. The threshold T varies between $[0.01,\ 10]$. The absolute difference percentage is shown in Fig. 7(b) and the optimal value of ρ^* for each threshold T in Fig. 7(c). These plots illustrate already significant gains from the pairwise geometric cooperation policies with the exchange of channel phase information between the transmitters. The absolute gain in coverage reaches a maximum of over 10% between $T = 0.1$ to 0.5. However the gains disappear for values of threshold $T > 2$ and the optimal policy is No Coop in the entire plane. The reason for the non-optimality of the cooperation policies - given the model under study - for high values of T can be found in the previous section of Pros and Cons.

C. Second Neighbour Interference Elimination by Dirty Paper Coding (DPC)

Significantly higher gains are obtained in the case where further knowledge over the channel state is available and exchanged at the transmission pair side. Specifically, the information over second neighbour interference may eliminate the negative effects from $\mathbf{b}_2$ and result in even higher coverage gains, apparent in the entire domain of T. Remember that, due to the far-field approximation, only $\mathbf{b}_2$ (and not $\mathbf{b}_1$) may cause interference at the typical location, due to service of its primary user. The improvement in coverage is illustrated in Fig. 7(d). Given the parameter values in our evaluation we get a maximum coverage gain of around 17% between $T = 0.2$ to 1. The absolute difference percentage is shown in Fig. 7(e) and the optimal value of ρ^* for each threshold T in Fig. 7(f).

VII. Conclusions and Future Work

In this paper, we have proposed a general methodology to treat problems of cooperation in cellular networks, in the case where data exchange is allowed only between pairs of nodes. The method can be easily extended however to the case of more than two cooperating BSs. The framework developed uses tools from stochastic geometry to model the random positions of nodes on the plane and calculate the network performance with reference to a typical location.

In our work the focus has been on the evaluation of the coverage probability, using a specific cooperation scheme. This scheme is based on the idea of conferencing by Willems, where two transmitters encode a common message after exchange of information over the backhaul. We give to the service of each user two possibilities, defined by a novel family of geometric policies. Either to be served by its closest BS or to ask from the two closest ones to cooperate. The latter choice splits the total user power between these two BSs, which encode the same common message. The scheme results in an additional term on the beneficial received signal due to the correlated nature of the two transmissions.

The treated cooperation scheme assumes only knowledge over the fast-fading angular shift at the cooperation pair. The purpose was to investigate possible coverage benefits, without the necessity of exhaustive channel state feedback and full-channel beamformer adaptation. Our method has revealed coverage benefits from cooperation, even in this case of limited channel information. The benefits are significantly improved when knowledge over second neighbour interference is taken into account and transmission is done using Dirty Paper Coding techniques.

The stochastic geometry framework introduce here, can be applied to the evaluation of other types of cooperation, as is the case where the transmitters have full knowledge of the instantaneous channel gains and adapt their functionality to it. Furthermore, the framework can be extended to include and investigate clusters of cooperation with a larger or unequal

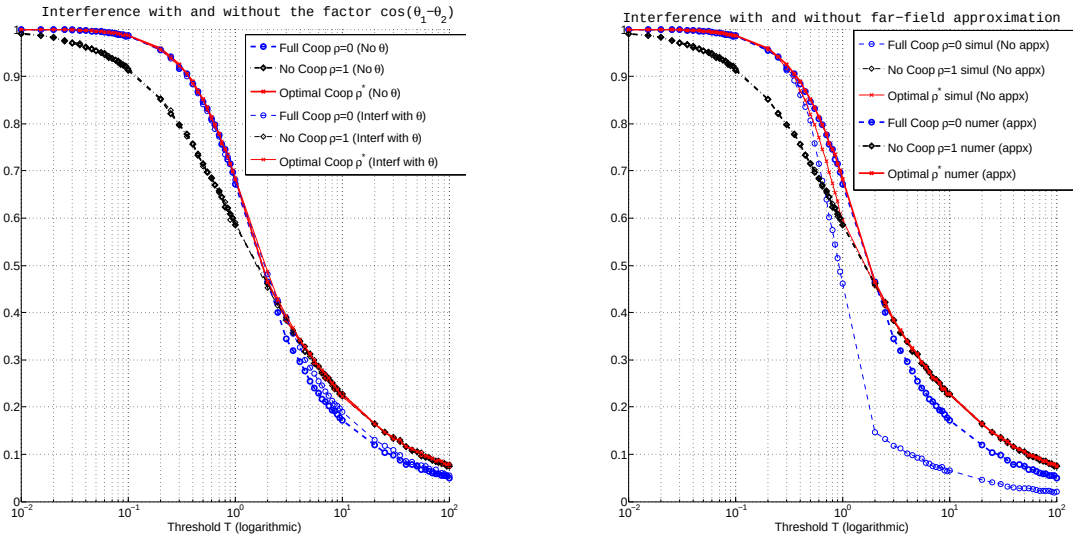

(a) With and without expectation over θ.

(b) With and without the far-field approximation.

Fig. 6. Pathloss exponent $\beta = 4$, user power $p = 1$. (a) Coverage probability comparison of two SINR models: with and without taking the expectation over $\cos(\theta_{n1,i} - \theta_{n2,i})$ for the interference. (b) Coverage probability comparison of two SINR models: with and without the far-field approximation ($d_{n1} \neq d_{n2}$) on the interference.

number of BSs, as well as variations of the type of point process used to model the BS topology on the plane. Treatment of such cases is very important, since it may reveal higher performance benefits, at the cost of more intensive information exchange at the transmitter side, and is an important future research direction.

ACKNOWLEDGEMENT

The authors would like to thank Konstantinos Manolakis (Heinrich Hertz Institute) and Namyoon Lee (UT Austin) for discussions over the subject and helpful comments that improved and clarified the presentation of the work.

APPENDIX A
NOTES ON THE MODEL

We use this Appendix to provide further clarifications on the model under study.

Association: Our work, which lets a typical user by served by one or two BSs in its proximity, generalizes the concept of associating the user to just to its closest BS, treated previously in [16]. The choice is made without considering fading, since the appropriate cluster is supposed to be kept the same for longer time-periods and the path-loss depends only on the user-BS distance.

Willems' scheme: This scheme has already been proposed and investigated for the case of cellular CoMP in [7] and [8], as well as for ad-hoc networks in [35] and [27]. We came here also to this choice, for two reasons. The first is that the scheme is *capacity achieving when no channel fading is considered at the model* [1], and the second is that it requires low information exchange. Of course in the CoMP case we do deal with fading. However the scheme is still beneficial compared to the case [36] where data flows add up orthogonally at the receiver. A better scheme in terms of coverage and throughput is the full-cooperation with interference cancellation within the cluster, but it comes at the expense of information exchange (full channel and data knowledge) and reservation of resources for a specific user of interest. In this sense, we believe that Willems' encoding offers the desired tradeoff between SINR gain and information feedback. To implement the scheme when fading is considered, the channel-phase needs to be known and exchanged between the cooperating transmitters. This technique is known in the literature as limited feedback beamforming with phase quantization, and is an attempt to co-phase the signal reception in the MISO case (see [37] and [38]).

Typical location: To avoid confusion, we remark that we apply here the tools of stochastic geometry at a typical location. Since in the point process analysis we treat random realizations of the BS topology, in some realizations the typical location will refer to a location close to the centre of its first neighbour, in others it will refer to a location at the cell edge. Such events have a frequency/probability that depends on the process distribution. The performance evaluation is in average over all such random deployments of the network on the plane.

APPENDIX B
PROOF OF LEMMA 3

For $i = 1, 2$, set $\mu_i := \frac{r_i^\beta}{p}$, so that the r.v. $X_i := g_i r_i^{-\beta}$ follows the exponential distribution $X_i \sim \exp(\mu_i)$ with $\mathbb{E}[X_i] = \frac{1}{\mu_i}$. We can easily conclude that the r.v. $\sqrt{X_i}$ follows the Rayleigh distribution with p.d.f.

$$f_{\sqrt{X_i}}(u) = 2\mu_i u e^{-\mu_i u^2}$$

and expected value $\mathbb{E}\left[\sqrt{X_i}\right] = \sqrt{\frac{\pi}{4\mu_i}}$. The p.d.f. of the sum of the two independent r.v.'s $\sqrt{Z} = \sqrt{X_1} + \sqrt{X_2}$ is given by

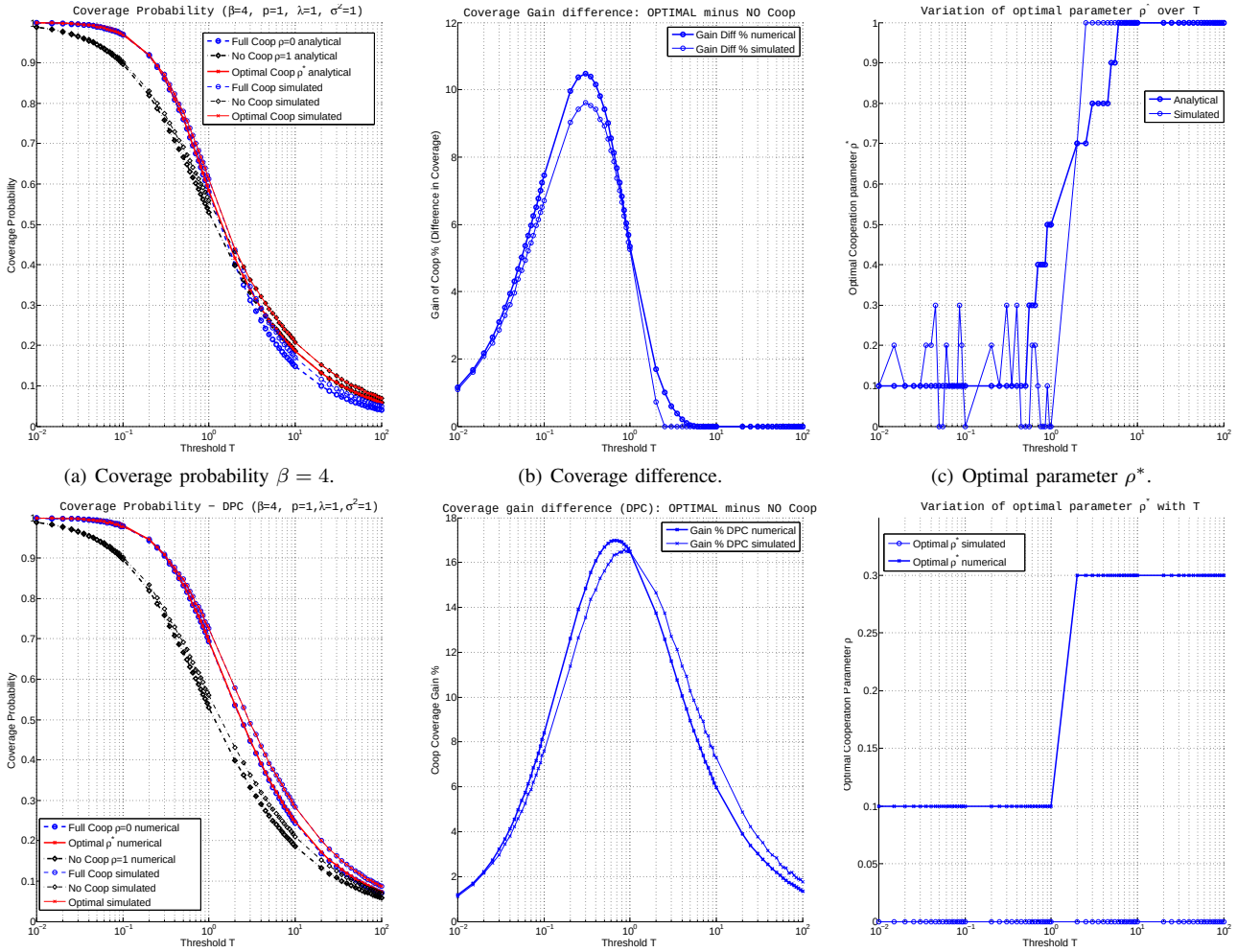

(a) Coverage probability $\beta = 4$. (b) Coverage difference. (c) Optimal parameter ρ^*.

(d) Coverage probability DPC $\beta = 4$. (e) Coverage difference DPC. (f) Optimal parameter ρ^* DPC.

Fig. 7. (a)-(c): Comparison between analytical and simulation results for coverage. Evaluation of the case $\beta = 4$ with far-field approximation./ Coverage improvement./ Optimal value of design parameter ρ^* for varying T. (d)-(e): Comparison between analytical and simulation results for coverage in the DPC case $\beta = 4$./ Coverage improvement./ Optimal value of ρ^* over T.

$$\begin{aligned}\mathcal{L}_{\mathcal{J}}(s,\rho,d_n) &= \mathbb{E}_{B_n}\left[\mathbb{E}_{G_n}\left[e^{-sd_n^{-\beta}G_nB_n}\right]\mathbb{E}_{G_{n1},G_{n2}}\left[e^{-sd_n^{-\beta}\frac{G_{n1}+G_{n2}}{2}(1-B_n)}\right]\right]\\ &= \rho^2\mathbb{E}_{G_n}\left[e^{-sd_n^{-\beta}G_n}\right]+\left(1-\rho^2\right)\mathbb{E}_{G_{n1},G_{n2}}\left[e^{-sd_n^{-\beta}\frac{G_{n1}+G_{n2}}{2}}\right]\\ &= \rho^2\mathcal{L}_G\left(sd_n^{-\beta}\right)+\left(1-\rho^2\right)\left(\mathcal{L}_G\left(\frac{sd_n^{-\beta}}{2}\right)\right)^2 \overset{(a)}{=} \rho^2\frac{1}{1+sd_n^{-\beta}p}+\left(1-\rho^2\right)\frac{1}{\left(1+sd_n^{-\beta}\frac{p}{2}\right)^2}. \end{aligned} \quad (35)$$

the convolution of their individual p.d.f.'s, namely

$$f_{\sqrt{Z}}(v) = 4\mu_1\mu_2\int_0^v u(v-u)\,e^{-\mu_1 u^2}e^{-\mu_2(v-u)^2}\,\mathrm{d}u.$$

Since we are interested in the p.d.f. of Z rather than of $\sqrt{Z}$ we make following observation. The first derivative of the cumulative distribution function (c.d.f.) of a r.v. Y is its p.d.f. $f_Y(y)$,

$$\mathbb{P}\left[Y^2 \le y\right] = \mathbb{P}\left[Y \le \sqrt{y}\right] \quad \Rightarrow \quad f_{Y^2}(y) = \frac{f_Y\left(\sqrt{y}\right)}{2\sqrt{y}}.$$

With the above transformation, we get the p.d.f. of Z directly from the convolution

$$\begin{aligned} f_Z(z) &= \frac{f_{\sqrt{Z}}\left(\sqrt{z}\right)}{2\sqrt{z}} = \\ &= \frac{4\mu_1\mu_2}{2\sqrt{z}}\int_0^{\sqrt{z}} u\left(\sqrt{z}-u\right)e^{-\mu_1 u^2}e^{-\mu_2\left(\sqrt{z}-u\right)^2}\,\mathrm{d}u. \end{aligned}$$

It can be verified that the p.d.f. is square integrable. Finally, the LT of Z

$$\mathcal{L}_Z(s) := \int_0^\infty e^{-sz}f_Z(z)\,\mathrm{d}z$$

is equal to the expression in (19), where $g(s) := \sqrt{1+\left(\frac{1}{\mu_1}+\frac{1}{\mu_2}\right)s}$. We can check that the resulting p.d.f. of Z is actually valid, since $\mathcal{L}_Z(0) = \int_0^\infty f_Z(z)\,\mathrm{d}z = 1$. The expected value of Z is found directly by the first derivative at $s=0$

$$\mathbb{E}[Z] = -\left.\frac{\mathrm{d}\mathcal{L}(s)}{\mathrm{d}s}\right|_{s=0}.$$

The expression is provided in (24) and an evaluation for $\mu_1 = \mu_2 = 1/2$ gives $\mathbb{E}[Z] = \pi + 4$.

Appendix C
Proof of Theorem 1

From the definition of the Laplace Transform we get for the Interference r.v.

$$\mathcal{L}_{\mathcal{I}}(s,\rho,r_2) = \mathbb{E}_{\mathcal{I}}\left[e^{-s\mathcal{I}}\right] =$$
$$\mathbb{E}_{\Phi,\{G_n\},\{G_{n1},G_{n2}\},\{B_n\}}\left[e^{-s\left(r_2^{-\beta}G_2B_2+r_2^{-\beta}\frac{G_1+G_2}{2}(1-B_2)\right)}\times\right.$$
$$\left.\times\prod_{\mathbf{z}_n\in\Phi\setminus\{\mathbf{b}_1,\mathbf{b}_2\}} e^{-s\left(d_n^{-\beta}G_nB_n+d_n^{-\beta}\frac{G_{n1}+G_{n2}}{2}(1-B_n)\right)}\right].$$

Observe now that the r.v.'s B_n, G_n, G_{n1}, G_{n2} are independently distributed and independent from the point process ϕ. The contribution of each atom outside the ball of radius r_2 is given by (35), where (a) comes fromt the LT of the random variable $G, G_n, G_{n1}, G_{n2} \sim \exp(1/p)$. Similarly for the atom on the boundary of the ball, the contribution is given from the above expression by replacing d_n by r_2. The LT of the interference finally can be expressed as

$$\mathcal{L}_{\mathcal{I}}(s,\rho,r_2) = \mathcal{L}_{\mathcal{J}}(s,\rho,r_2)\,\mathbb{E}_\Phi\left[\prod_{\mathbf{z}_n\in\Phi\setminus\{\mathbf{b}_1,\mathbf{b}_2\}}\mathcal{L}_{\mathcal{J}}(s,\rho,d_n)\right]$$
$$\stackrel{(b)}{=} \mathcal{L}_{\mathcal{J}}(s,\rho,r_2)\,e^{-2\pi\lambda\int_{r_2}^\infty(1-\mathcal{L}_{\mathcal{J}}(s,\rho,r))r\,\mathrm{d}r},$$

where (b) comes from applying the Laplace functional expression for the p.p.p. using polar coordinates [29, Prop. 1.5, pp. 18-19], for radius r ranging from r_2 to ∞, since it has already been identified that the second closest neighbour lies at the boundary of the ball of radius r_2.

Appendix D
Proof of Theorem 2

The probability of coverage in (20), given the SINR expression in (18) can be broken into two separate integrals $q_c(\rho) = q_{c,1}(\rho) + q_{c,2}(\rho)$, which should be further calculated.

$$q_c(\rho) = \mathbb{E}_{r_1,r_2}\left[\mathbb{P}\left[\mathrm{SINR}(\rho,r_1,r_2) > T | r_1,r_2\right]\right]$$
$$= \int_0^\infty\int_{\frac{r_1}{\rho}}^\infty \mathbb{P}\left[G_1 > r_1^\beta T\left(\sigma^2+\mathcal{I}\right)|r_1,r_2\right] f_{r_1,r_2}\,\mathrm{d}r_2\,\mathrm{d}r_1$$
$$+\int_0^\infty\int_{r_1}^{\frac{r_1}{\rho}} \mathbb{P}\left[Z_{r_1,r_2} > 2T\left(\sigma^2+\mathcal{I}\right)|r_1,r_2\right] f_{r_1,r_2}\,\mathrm{d}r_2\,\mathrm{d}r_1,$$

where the Z_{r_1,r_2} r.v. is defined in (23). For the first integral we derive the probability expression

$$\mathbb{P}\left[G_1 > r_1^\beta T\left(\sigma^2+\mathcal{I}\right)|r_1,r_2\right] \stackrel{(a)}{=}$$
$$\mathbb{E}_{\mathcal{I}}\left[\mathbb{P}\left[G_1 > r_1^\beta T\left(\sigma^2+\mathcal{I}\right)|r_1,r_2,\mathcal{I}\right]\right] \stackrel{(b)}{=}$$
$$\mathbb{E}_{\mathcal{I}}\left[e^{-\frac{r_1^\beta}{p}T\left(\sigma^2+\mathcal{I}\right)}|r_1,r_2\right] \stackrel{(c)}{=}$$
$$e^{-\frac{r_1^\beta}{p}T\sigma^2}\mathcal{L}_{\mathcal{I}}\left(\frac{r_1^\beta}{p}T,\rho,r_2\right).$$

In the above, (a) comes from the law of total probability, (b) from the fact that $G_1 \sim \exp(1/p)$ and (c) from the definition of the Laplace transform.

For the second integral, we will use the Proposition in [29, Prop.5.4] or alternatively in [39, Prop.2.2] for the expression of the coverage probability for general fading. The conditions to apply the proposition is that Z_{r_1,r_2} has a finite first moment and admits a square integrable density (shown in Lemma 3 and that $\mathcal{I}$ admits a square integrable density. Then we get that

$$\mathbb{P}\left[Z_{r_1,r_2} > 2T\left(\sigma^2+\mathcal{I}\right)|r_1,r_2\right] =$$
$$\int_{-\infty}^\infty e^{-2j\pi\sigma^2 s}\mathcal{L}_{\mathcal{I}}(2j\pi s,\rho,r_2)\,\frac{\mathcal{L}_Z\left(-j\pi s/T,\frac{r_1^\beta}{p},\frac{r_2^\beta}{p}\right)-1}{2j\pi s}\,\mathrm{d}s,$$

where $\mathcal{L}_Z(s,\mu_1,\mu_2)$ is the LT of the general fading r.v. Z_{r_1,r_2}, whose expression is provided in (19) and $\mathcal{L}_{\mathcal{I}}(s,\rho,r_2)$ is the LT of the interference r.v. $\mathcal{I}$, provided in (28). In the case of DPC, the LT for the interference r.v. is provided in (33). Substituting the probability expressions in $q_{c,1}(\rho)$ and $q_{c,2}(\rho)$ respectively and using the joint distribution over r_1, r_2 from (21) in Lemma 1, we conclude the proof.

References

[1] F. M.J. Willems. The discrete memoryless Multiple Access Channel with partially cooperating encoders. *IEEE Trans. on Information Theory*, IT-29:441–445, May 1983.

[2] Moritz Wiese, Holger Boche, Igor Bjelakovic, and Volker Jungnickel. The Compound Multiple Access Channel with partially cooperating encoders. *IEEE Trans. on Information Theory*, 57, no. 5:3045–3066, May 2011.

[3] S. I. Bross, A. Lapidoth, and M. A. Wigger. The Gaussian MAC with conferencing encoders. *IEEE International Symposium on Information Theory (ISIT)*, pages 2702–2706, 2008.

[4] M. K. Karakayali, G. J. Foschini, and R. A. Valenzuela. Network coordination for spectrally efficient communications in cellular systems. *IEEE Wireless Communications Mag.*, 13, no.4:56–61, Aug. 2006.

[5] D. Lee, H. Seo, B. Clerckx, E. Hardouin, D. Mazzarese, S. Nagata, and K. Sayana. Coordinated multipoint transmission and reception in LTE-advanced: Deployment scenarios and operational challenges. *IEEE Communications Magazine*, 50, issue: 2:148–155.

[6] D. Gesbert, S. Hanly, H. Huang, S. Shamai Shitz, O. Simeone, and W. Yu. Multi-cell MIMO cooperative networks: A new look at interference. *IEEE JSAC*, 28, no.9:1–29, Dec. 2010.

[7] R. Zakhour and D. Gesbert. Optimized data sharing in multicell MIMO with finite backhaul capacity. *IEEE Trans. on Signal Processing*, 59, iss. 12:6102–6111, Dec. 2011.

[8] P. Marsch and G. Fettweis. On base station cooperation schemes for downlink network MIMO under a constrained backhaul. *IEEE Globecom*, 2008.

[9] A. Giovanidis, J. Krolikowski, and S. Brueck. A 0-1 program to form minimum cost clusters in the downlink of cooperating base stations. *Proc. of the Wireless Communications and Networking Conference (WCNC), Paris, France*, Apr. 2012.

[10] A. Papadogiannis, D. Gesbert, and E. Hardouin. A dynamic clustering approach in wireless networks with multi-cell cooperative processing. *IEEE ICC*, 2008.

[11] P. de Kerret and D. Gesbert. Sparse precoding in multicell MIMO systems. *Proc. of the Wireless Communications and Networking Conference (WCNC), Paris, France*, April 2012.

[12] E. Björnson and E. Jorswieck. *Optimal Resource Allocation in Coordinated Multi-Cell Systems*. Now Publishers Inc, Foundations and Trends in Communications and Information Theory, Vol. 9: No 2-3, pp 113-381, 2013.

[13] P. de Kerret and D. Gesbert. CSI sharing strategies for transmitter cooperation in wireless networks. *IEEE Wireless Communications*, pages 43–49, Feb. 2013.

[14] V. Jungnickel, K. Manolakis, S. Jaeckel, M. Lossow, P. Farkas, M. Schlosser, and V. Braun. Backhaul requirements for Inter-site cooperation in heterogeneous LTE-advanced networks. *IEEE ICC, Budapest, Hungary*, June 2013.

[15] D. Jaramillo-Ramirez, M. Kountouris, and E. Hardouin. Coordinated multi-point transmission with quantized and delayed feedback. *In: Proc. IEEE GLOBECOM*, pages 2391–2396, 2012.

[16] J. G. Andrews, F. Baccelli, and R. K. Ganti. A tractable approach to coverage and rate in cellular networks. *IEEE Trans. on Communications*, 59, issue: 11:3122–3134, 2011.

[17] H. S. Dhillon, R. K. Ganti, F. Baccelli, and J. G. Andrews. Modeling and analysis of K-Tier downlink heterogeneous cellular networks. *IEEE Journal on Selected Areas in Communications*, 30, no. 3:550–560, April 2012.

[18] B. Błaszczyszyn, M.K. Karray, and H.P. Keeler. Using Poisson processes to model lattice cellular networks. *In: Proc. IEEE INFOCOM 2013, Turin, Italy*, pages 773–781, April 2013.

[19] S. Akoum and R. W. Heath Jr. Interference coordination: Random clustering and adaptive limited feedback. *IEEE Trans. on Signal Processing*, 61, no. 7:1822–1834, April 2013.

[20] K. Huang and J.G. Andrews. An analytical framework for multicell cooperation via stochastic geometry and large deviations. *IEEE Trans. Info. Theory*, 59, no. 4:2501–2516, April 2013.

[21] F. Baccelli and A. Giovanidis. Coverage by pairwise base station cooperation under adaptive geometric policies. *In Proc. of the 47th Annual Asilomar Conference on Signals, Systems and Computers, Monterey, USA.*, Nov. 2013.

[22] G. Nigam, P. Minero, and M. Haenggi. Coordinated multipoint in heterogeneous networks: A stochastic geometry approach. *In: Proc. IEEE GLOBECOM Workshop on Emerging Technologies for LTE-Advanced and Beyond 4G (GLOBECOM-B4G'13), Atlanta, GA*, Dec. 2013.

[23] R. Tanbourgi, S. Singh, J.G. Andrews, and F.K. Jondral. A tractable model for non-coherent joint-transmission base station cooperation. *arXiv:1308.0041 [cs.IT]*, Feb. 2014.

[24] B. Błaszczyszyn and H.P. Keeler. Studying the SINR process of the typical user in poisson networks by using its factorial moment measures. *arXiv:1401.4005 [cs.NI]*, Jan. 2014.

[25] D.-T. Lee. On k-nearest neighbor Voronoi diagrams in the plane. *IEEE Trans. on Computers*, c-31, no. 6:478–487, June 1982.

[26] M. de Berg, O. Cheong, M. van Kreveld, and M. Overmars. *Computational Geometry: Algorithms and Applications*. Springer-Verlag, 3rd rev. ed. 2008.

[27] A. Sendonaris, E. Erkip, and B. Aazhang. User cooperation diversity - part I: System description. *IEEE Trans. on Comm.*, 51, no. 11:1927–1938, Nov. 2003.

[28] R.K. Ganti, Z. Gong, M. Haenggi, C. Lee, S. Srinivasa, D. Tisza, S. Vanka, and P. Vizi. Implementation and experimental results of superposition coding on software radio. *IEEE International Conference on Communications (ICC)*, 2010.

[29] F. Baccelli and B. Błaszczyszyn. *Stochastic Geometry and Wireless Networks vol. I & II*. now Publishers Inc. - Foundations and Trends in Networking 3:3-4, 2009.

[30] G. Last and H. Thorisson. What is typical? *J. Appl. Prob. Spec. Vol. 48A, 379-389*, 2011.

[31] A. Alzaid, J.S. Kim, and F. Proschan. Laplace ordering and its applications. *J. Appl. Prob.*, 28:116–130, 1991.

[32] S. Asmussen. *Applied Probability and Queues*. Springer-Verlag, 2003.

[33] M. H. M. Costa. Writing on Dirty Paper. *IEEE Trans. on Information Theory*, IT-29, no. 3:439–441, May 1983.

[34] G. Caire and S. Shamai (Shitz). On the achievable throughput of a multiantenna Gaussian broadcast channel. *IEEE Trans. on Information Theory*, 49, no. 7:1691–1706, July 2003.

[35] J. N. Laneman, D.N.C. Tse, and G.W. Wornell. Cooperative diversity in wireless networks: Efficient protocols and outage behavior. *IEEE Trans. Info. Theory*, 50, no.12:3062–3080, Dec. 2004.

[36] S. Shabdanov, P. Mitran, and C. Rosenberg. On cooperative wireless relaying: A joint routing and scheduling flow-based framework. *In: Proc. IEEE GLOBECOM*, pages 4641–4646, 2012.

[37] R. W. Heath and A. Paulraj. A simple scheme for transmit diversity using partial channel feedback. *In. Proc. IEEE Asilomar Conf. on Signals, Systems, and Comp.*, 2:1073–1078, Nov. 1998.

[38] D.J. Love, R.W. Heath Jr., V.K.N. Lau, D. Gesbert, B.D. Rao, and M. Andrews. An overview of limited feedback in wireless communication systems. *IEEE JSAC*, 26, no. 8:1341–1365, Oct. 2008.

[39] F. Baccelli, B. Błaszczyszyn, and P. Muhlethaler. Stochastic analysis of spatial and opportunistic Aloha. *IEEE JSAC*, 27, no.7:1105–1119, Sept. 2009.